JOURNAL OF VIROLOGY, Dec. 2005, p. 15376–15387 Vol. 79, No. 24
0022-538X/05/$08.00+0 doi:10.1128/JVI.79.24.15376–15387.2005

Division of Labor within Human Immunodeficiency Virus Integrase Complexes: Determinants of Catalysis and Target DNA Capture†

Tracy L. Diamond and Frederic D. Bushman*

University of Pennsylvania School of Medicine, Department of Microbiology, 3610 Hamilton Walk, Philadelphia, Pennsylvania 19104-6076

Received 20 July 2005/Accepted 27 September 2005

Following the completion of reverse transcription, the human immunodeficiency virus integrase (IN) enzyme covalently links the viral cDNA to a host cell chromosome. An IN multimer carries out this reaction, but the roles of individual monomers within the complex are mostly unknown. Here we analyzed the distribution of functions for target DNA capture and catalysis within the IN multimer. We used forced complementation between pairs of IN deletion derivatives in vitro as a tool for probing *cis-trans* relationships and analyzed amino acid substitutions affecting either catalysis or target site selection within these complementing complexes. This allowed the demonstration that the IN variant contributing the active catalytic domain was also responsible for recognition of the integration target DNA. We were further able to establish that a single monomer is responsible for both functions by use of assay mixtures containing three different IN genotypes. These data specify the ligands bound at the catalytically relevant IN monomer and allow more-specific modeling of the mechanism of inhibitors that also bind this surface of IN.

Many DNA-modifying enzymes act as homomultimers, in which different monomers contribute separate functions during the overall reaction cycle (3, 10). For example, during phage Mu transposition, different monomers within a tetramer of the Mu A transposase carry out covalent chemistry and binding of the Mu B cofactor (2, 38). In the tyrosine recombinase family, single monomers of the Cre enzyme contribute both the active-site tyrosine and the activating catalytic residues (23), whereas for the related Flp recombinase, the two functions are contributed by two separate monomers in *trans* (35). Here we investigate a related issue for the human immunodeficiency virus (HIV) integrase (IN) complex, i.e., whether the catalytic residues and the target site selection function are contributed by the same or different IN monomers within the active IN multimer.

The retroviral IN enzyme carries out the initial DNA-breaking and -joining reactions involved in integration (3, 9). After reverse transcription of the viral RNA to produce double-stranded cDNA, IN cleaves two nucleotides from each 3′ end of the viral cDNA (terminal cleavage; Fig. 1A, part 1). The recessed 3′ hydroxyl groups are then joined to phosphodiester bonds in the cellular target DNA (strand transfer; Fig. 1A, part 2). In vitro, recombinant IN is able to carry out the terminal cleavage and strand transfer reactions (3, 9). IN is also able to carry out disintegration, a reversal of the strand transfer reaction (Fig. 1A, part 3) (8).

Retroviral IN proteins are composed of three domains (Fig. 1B). Structures of each IN domain have been determined in isolation (11, 21, 22), as have the structures of two-domain fragments (6, 7, 45, 46). However, the structures of the entire IN enzyme and of IN in complex with substrate DNA have not been solved. Interactions with viral and target DNA have been mapped by cross-linking studies (reviewed in reference 18), and functions of different domains have been mapped by mutagenesis (reviewed in reference 12).

Based on their catalytic domain sequences, the retroviral INs can be grouped into a large family of polynucleotide phosphotransferase enzymes that include RuvC, bacterial and retroviral RNaseHs, and a variety of bacterial transposases (reviewed in references 3 and 10). The catalytic domain (amino acid residues 50 to 212 [50-212]) contains a conserved $D,DX_{35}E$ motif that coordinates the metal ions, Mn^{2+} or Mg^{2+}, that mediate catalysis (14, 19, 42). The catalytic domain also specifies the choice of target DNA sequences for integration in vitro, as shown by the identification of amino acid substitutions at residue 119 in HIV IN that alter the pattern of favored sites. Similar results have been obtained for several other retroviral IN proteins (1, 24, 25, 31, 32, 41).

The N-terminal domain (residues 1-50) contains a conserved HHCC motif within a helix-turn-helix-like fold and appears to contribute to DNA binding (28). The C-terminal domain (residues 220-270) has an SH3-like fold and also contributes to DNA binding (16, 18, 28). The catalytic domain and the C-terminal domain are connected by an alpha-helical linker (12-220). The last few residues of IN (270-288) are disordered in available structures and are of uncertain function. Deletion of either the N- or C-terminal domain strongly impairs the terminal cleavage and strand transfer activities, but the catalytic domain alone can carry out the disintegration reaction (5, 44).

Mixing together truncated IN derivatives (e.g., 1-212 plus 50-288) can restore terminal cleavage and strand transfer activity in vitro and in vivo (Fig. 1B, row 7) (13, 17, 36, 43). This indicates that IN acts as a multimer during terminal cleavage and strand transfer, consistent with physical data indicating that IN can form higher-order complexes (6, 11, 30, 45). In these complementing pairs, substitutions that block catalysis

* Corresponding author. Mailing address: University of Pennsylvania School of Medicine, Department of Microbiology, 3610 Hamilton Walk, Philadelphia, PA 19104-6076. Phone: (215) 573-8732. Fax: (215) 573-4856. E-mail: bushman@mail.med.upenn.edu.

† Supplemental material for this article may be found at http://jvi.asm.org.

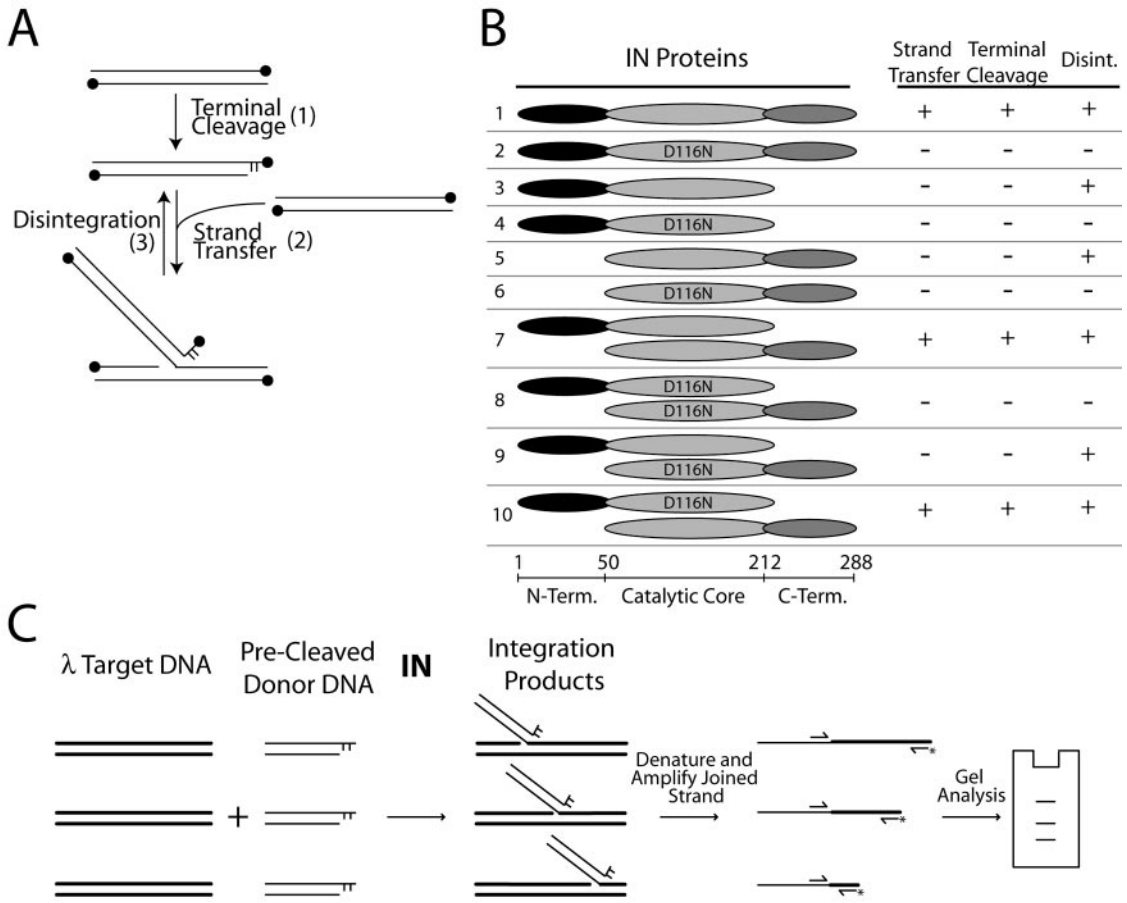

FIG. 1. Integrase and the integration reaction. (A) Diagram of the activities of integrase on oligonucleotide substrates matching the viral DNA end. See text for details. 5′ ends of oligonucleotides are depicted by black dots. (B) Complementation between derivatives of IN (13, 43). Ovals are used to depict the N-terminal (black), catalytic (light gray), and C-terminal (dark gray) domains. The ability to carry out strand transfer, terminal cleavage, and/or disintegration (disint.) is indicated by +. (C) Diagram of the PCR-based in vitro integration assay. Lambda target DNA was mixed with IN and an oligonucleotide matching the precleaved viral DNA end was then added to start the reaction. Integration products were then denatured and amplified using (i) a primer complementary to the donor DNA and (ii) [^{32}P]ATP-labeled primer complementary to the lambda target DNA. Amplified products were analyzed by gel electrophoresis.

(e.g., D116N) are tolerated in the 1-212 partner but not the 50-288 partner (Fig. 1B, compare rows 9 and 10). Thus, the complementation data indicate that IN forms multimers and that the 50-288 IN partner donates the active catalytic domain. The number of IN monomers normally present in active multimers has not been fully clarified due to the poor solubility of IN under the low-salt conditions required to support activity in vitro.

Complementation has also been shown to occur between HIV integrase mutants during HIV infection in vivo (17, 37). In one recent study, mutants in the active site and mutants potentially affecting DNA binding did not show complementation, suggesting that these activities reside in the same integrase complementation group.

In order to test the role of the different IN monomers within active multimers, we have introduced amino acid substitutions affecting catalysis and target site specificity into complementing pairs of HIV type 1 (HIV-1) IN derivatives and assayed the mixtures for strand transfer activity and target sequence preferences. Initially, this revealed that target site selection was dictated by the genotype of the 119 residue within the catalytically active 50-288 partner and not by the 1-212 partner. However, this result alone does not specify whether a single 50-288 monomer was responsible for both functions or whether one contributed the catalytic activity and another the target-specifying function. We thus assayed mixtures containing three different truncated IN proteins, one 1-212 derivative and two different 50-288 derivatives, which revealed that the target specification function was determined by the catalytically active 50-288 monomer. This supported a model in which a single monomer was responsible for both catalysis and target site selection (at the single viral DNA end probed in these experiments). This work allows us to specify the roles of IN monomers within the IN-DNA complex and has implications for understanding the action of IN inhibitors that bind the catalytic domain.

MATERIALS AND METHODS

Construction of mutant IN. All DNA oligonucleotides used are summarized in Table S1 in the supplemental material. To generate HIV-1 NL43 IN with the

F185H substitution (referred to as wild-type IN), EcoRI/EcoRV fragment containing the substitution transferred from the pH1IN5 to the pH1IN1 plasmid (18), yielding pINF185H6. The D116N mutation was introduced by transferring an XhoI/EcoRI fragment from pH1IN14 plasmid (18), which contained the D116N substitution, to pINF185H6. S119A and S119D mutants were generated by PCR-based site-directed mutagenesis using the 2598-2617 F primer and the appropriate mutation-containing primer (S119A SpeI R, S119A D116N SpeI R, S119D SpeI R, or S119D D116N SpeI R). The IN coding regions were cloned into the pDuetMxe expression vector by use of NdeI and BsrGI after amplifying the IN gene with the NL43 IN1 NdeI F and NL43 IN288 BsrGI R primers. In this vector, the INs were cloned amino terminally to an Mxe intein, a chitin binding domain, and a hexahistidine tag for purification.

For 1-212 truncations, plasmids were restricted with EcoRV and BamHI and ligated to annealed IN212 cut F and IN212 cut R primers in order to replace the end of the IN coding region and introduce an ochre stop after codon 212. The 50-288 truncations were generated by amplifying the various IN coding regions with the IN50 NsiI F and 3100-3084 R primers and cloning NsiI/EcoRV-restricted fragments back into the original vectors.

Protein expression and purification. IN constructs were transformed into BL21-CodonPlus(DE3)-RIL *Escherichia coli* cells (Stratagene, Calif.), and protein expression was induced with 150 μM IPTG (isopropyl-β-D-thiogalactopyranoside) at an optical density at 600 nm of 0.5. After 3 h at 37°C, cells were harvested and pellets were flash frozen in liquid nitrogen and stored at −80°C.

For full-length IN clones in the pDuetMxe vector, pellets were resuspended in Ni lysis buffer (50 mM Na, KPO_4 [pH 8], 300 mM NaCl) and lysed with lysozyme (1.7 mg/ml). Proteinase inhibitor cocktail I (1×; Calbiochem, Calif.) and 10 mM CHAPS {3-[(3-cholamidopropyl)-dimethylammonio]-1-propanesulfonate} (Sigma-Aldrich, Mo.) were added and lysates sonicated. Lysates were cleared by centrifugation and passed through a 0.45-μM filter and loaded onto a column of Ni-nitrilotriacetic acid agarose (Invitrogen, Calif.) that was previously equilibrated with Ni lysis buffer. Columns were washed with Ni wash buffer (50 mM Na, KPO_4 [pH 8], 300 mM NaCl, 10 mM CHAPS, 10 mM imidazole), and protein was eluted with Ni elution buffer (50 mM Na, KPO_4 [pH 9], 300 mM NaCl, 10 mM CHAPS, 250 mM imidazole). Eluent was loaded onto a chitin column (New England BioLabs, Mass.) equilibrated with chitin wash buffer (CWB; 20 mM Na-HEPES [pH 8], 300 mM NaCl, 0.1 mM EDTA, 10 mM CHAPS). The column was washed with CWB and eluted with CWB plus 50 mM dithiothreitol. Buffer exchange was carried out using a YM-30 Centriprep instrument to transfer the protein into IN storage buffer (ISB; 20% glycerol, 727 mM NaCl, 7.27 mM HEPES [pH 7.5], 7.27 mM β-mercaptoethanol [β-ME], 7.27 μM $ZnSO_4$).

Truncated proteins were purified containing an amino-terminal hexahistidine tag. Cell pellets from induced cultures were resuspended in lysis buffer (20 mM Tris HCl [pH 7.9], 200 mM NaCl) and lysed with 2 mg/ml lysozyme. Proteinase inhibitor cocktail I (1×; Calbiochem, Calif.) and 10 mM CHAPS (Sigma-Aldrich, Mo.) were added, and the solution was brought to 1 M NaCl, 5 mM β-ME, and 5 mM imidazole. The lysate was then sonicated and cleared by centrifugation and passage through a 0.45-μM filter. The sample was loaded onto a Ni-nitrilotriacetic acid agarose resin that was previously equilibrated with binding buffer (1 M NaCl, 20 mM Tris HCl [pH 7.9], 5 mM β-ME, 10 mM CHAPS, 10 mM imidazole). The column was washed with binding buffer and wash buffer (1 M NaCl, 20 mM Tris HCl [pH 7.0], 5 mM β-ME, 10 mM CHAPS, 25 mM imidazole). Finally, the column was eluted with elution buffer (1 M NaCl, 20 mM Tris HCl, 5 mM β-ME, 10 mM CHAPS, 0.2 M imidazole), and buffer exchange was completed into ISB (see above).

PCR-based in vitro integration assay. The PCR-based in vitro integration assay was carried out as described in reference 4. Purified IN variants were diluted to 10 pmol/μl in ISB (see above), and 30 pmol (or 15 pmol of each IN derivative in double mixtures or 15 pmol of 1-212 and 7.5 pmol of each of two 50-288 derivatives in triple mixtures) was incubated with 3 μg of lambda DNA/HindIII (target DNA; Invitrogen, Mass.) in 25 mM KCl, 10 mM β-ME, 30 mM MES (morpholineethanesulfonic acid; pH 6.7), 15 mM $MnCl_2$, 10% glycerol, and 0.1 mg/ml bovine serum albumin. Reactions were initiated with 3 pmol of annealed FB-64/FB65-2 substrate. Reaction mixtures were incubated at 37°C for 30 min, and reactions were stopped with the addition of proteinase K (Roche, N.J.) and sodium dodecyl sulfate and incubation at 37°C for 45 min and 60°C for 3 min. Strand transfer products were purified using a Qiaquick PCR purification kit (QIAGEN, Calif.) and were eluted in 30 μl elution buffer. Five-μl portions were used as templates in PCRs. For these PCRs, one primer (FB66) was directed toward the oligonucleotide donor DNA (FB-64/FB65-2), and the other was labeled at the 5′ end with [γ-^{32}P]ATP and complementary to either the top (FB183) or bottom (FB182) strand of the lambda DNA/HindIII target. PCR products were analyzed by 6% polyacrylamide-urea gel electrophoresis (Sequagel; National Diagnostics, Ga.) and by use of a PhosphorImager (GE Healthcare, N.J.). Bands were quantified using ImageQuant software (GE Healthcare).

Oligonucleotide assays for IN activity. Oligonucleotide assays for terminal cleavage, strand transfer, and disintegration were adapted from those described in reference 18. IN stocks were diluted in ISB so that the concentrations in reaction mixtures would be 4 μM full-length IN, 4 μM 1-212 truncated IN, 2 μM 50-288 truncated IN, or a mixture of 4 μM 1-212 and 2 μM 50-288 truncated INs. Reactions were performed with 20 μM HEPES (pH 7.5), 1.8 μM β-ME, 10 μM $MnCl_2$, 30 nM ^{32}P-labeled substrate DNA, and, for strand transfer and terminal cleavage reactions, 30 nM unlabeled substrate DNA. Reactions were stopped by 10-fold dilution in formamide loading buffer (80% [wt/vol] deionized formamide, 10 mM EDTA [pH 8], 1 mg/ml xylene cyanol FF, 1 mg/ml bromophenol blue) and incubation at 95°C for 5 min. Reactions were analyzed by use of 6% polyacrylamide-urea gels and visualized with a Molecular Dynamics Storm PhosphorImager.

RESULTS

IN mutants used in this study. In order to examine the relationship between catalytic activity and target site specificity, the D116N, S119A, and S119D substitutions were introduced into deletion derivatives of the HIV-1 NL43 *IN* coding region by site-directed mutagenesis. Previous studies have shown that the D116N substitution, which is part of the highly conserved D,DX_{35}E motif, eliminates catalytic functions of the enzyme (reviewed in reference 12). As discussed above, substitutions of S119 alter target site specificity, thereby allowing us to follow the monomer responsible for contacting target DNA (24, 25, 34). Full-length INs (1-288) and truncated variants (1-212 or 50-288) were cloned and purified after overexpression in *E. coli* using affinity tags.

PCR assay of strand transfer activity in vitro. A PCR-based method was used to assay integration in vitro (Fig. 1C) (33, 40), because the PCR step allowed sensitive detection of products, which was needed as described below, and many sites in target DNA could be analyzed in a single experiment. Full-length IN or complementing mixtures were incubated with phage lambda target DNA, and then the reaction was initiated by addition of an oligonucleotide duplex matching the viral DNA end. Strand transfer products were amplified by PCR using one primer complementary to the viral DNA end and the other complementary to a strand of the lambda target DNA. Separate assays were carried out to monitor integration in each of the two target DNA strands. The 5′ end of the target DNA primer was end labeled with [^{32}P]ATP. PCR products were then analyzed by gel electrophoresis and autoradiography. Thus, each band on the final gel represents integration at a particular phosphodiester in the target DNA.

Complementation among IN mutants. Strand transfer was next tested with truncated forms of the two IN mutants and as complementing pairs. Reactions with the full-length IN (1-288) yielded strand transfer products indicated as a ladder of bands on the gels (Fig. 2A and B, lanes 2). In contrast, IN 1-288 containing the D116N substitution was not able to catalyze strand transfer detectably, as expected (Fig. 2A and B, lanes 3, "N"). Reactions with deleted derivatives IN 1-212 (Fig. 2A and B, lanes 4) and IN 50-288 (Fig. 2A and B, lanes 6) yielded much less product than reactions with the full-length INs. The PCR assay is much more sensitive than the oligonucleotide assays previously used to assay complementation, where no strand transfer activity was seen with these enzyme truncations alone (13, 43). In the PCR assay, reactions with IN 50-288

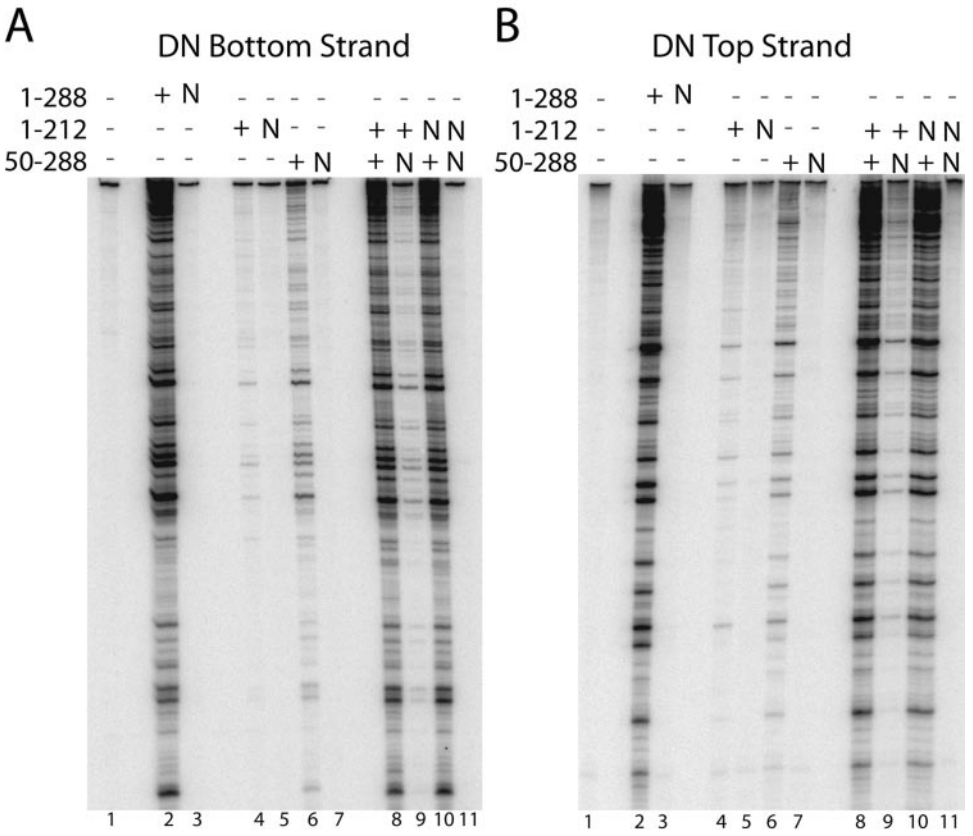

FIG. 2. Complementation in vitro among IN mutants analyzed using a PCR-based method. (A) Assays of integration into the top strand of a phage lambda DNA target. (B) Assays of integration into the bottom strand of a phage lambda DNA target. Full-length (1–288), C-terminally truncated (1–212), or N-terminally truncated (50–288) proteins were used in the PCR-based in vitro integration assay either alone or in the mixtures indicated above the autoradiogram. Lane 1 depicts a negative control where all steps were performed but no IN was added. +, wild-type sequence; "N," D116N catalytic mutant.

reproducibly yielded low but detectable levels of product. The truncations containing the D116N substitution did not display any detectable activity (Fig. 2A and B, lanes 5 and 7).

In Fig. 2A and B, lanes 8 to 11 show products of reactions with mixtures of IN 1-212 and IN 50-288. As expected, some mixtures showed complementation in vitro; that is, there was considerably more product from reactions with the mixtures than from those with either protein individually. Complementation was detected when neither protein had the D116N catalytic substitution (lane 8) or when only the IN 1-212 partner had the catalytic substitution (lane 10) but not when the catalytic substitution was present in the IN 50-288 partner (lane 9) or in both (lane 11). These results with the PCR-based assay confirm previous studies (13, 43) and imply that the catalytic domain carrying out catalysis is donated by the IN 50-288 derivative.

Modulation of target site specificity by the S119A substitution. In order to investigate which catalytic domain in a complementing pair is responsible for recognizing the target DNA, we introduced the S119A substitution, which alters favored target DNA sequences (24, 25, 34), into the deletion derivatives shown in Fig. 1B. The PCR-based in vitro integration assay was used to analyze strand transfer and target site specificity. As seen in Fig. 3A, lanes 2 and 4, and C, lanes 3 and 5, the full-length protein containing the S119A substitution ("A") has a pattern of strong and weak bands (target sites) different from that of the wild-type IN (+). This experiment was repeated, and patterns were highly reproducible.

In order to quantify patterns observed, two bands with differences between + and A were chosen and quantified by PhosphorImager analysis. The ratio of the intensities of the bands was determined and plotted (Fig. 3B and D). Quantitative analysis was carried out only for reactions that showed increased product formation for the complementing pairs compared to that for either of the truncated proteins alone. For the SA top strand reactions, the ratio of the intensity of band α to that of band β (Fig. 3B) for + was ~2, while the ratio for A was ~1. For the SA bottom strand reactions (Fig. 3D), another pair of bands was chosen (γ and δ), and the γ/δ ratio for + was between 1 and 2, while the ratio for A was 0.2 to 0.4. For each autoradiogram presented, two additional pairs of bands were also quantified and found to yield similar conclusions (data not shown). Thus, the PCR assay readily reveals differences in target site selection due to changes at residue 119.

Use of S119A to identify the complementing partner controlling target site specificity. We next carried out complementation assays to determine whether the same IN mutant donated both the catalytic and the target-specifying activities. To

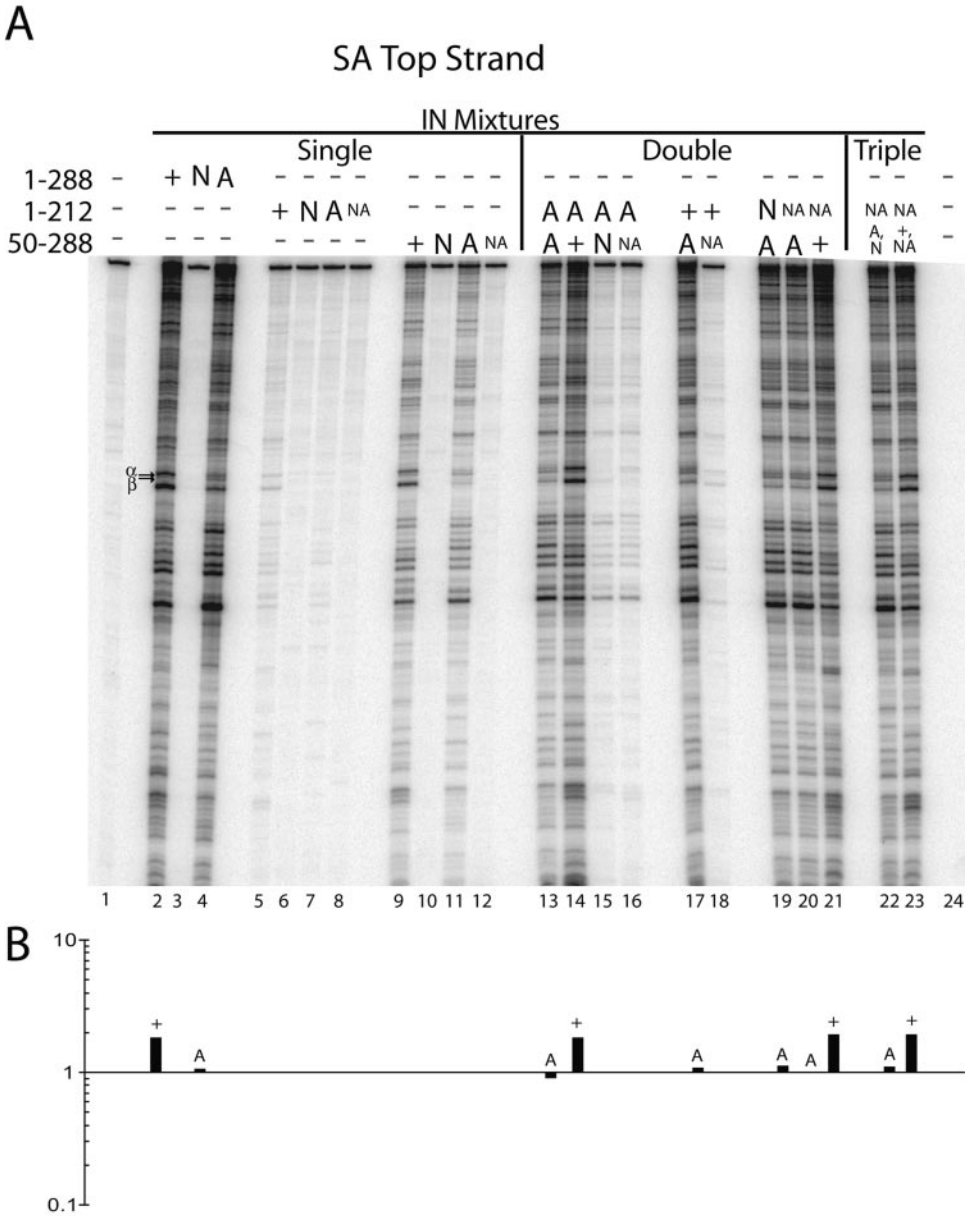

FIG. 3. Complementation assays in vitro containing S119A indicate that the 50–288 partner is responsible for both target sequence recognition and catalysis. (A) Assays of integration into the top strand of a phage lambda DNA target. Full-length (1–288), C-terminally truncated (1–212), or N-terminally truncated (50–288) proteins were used in the PCR-based in vitro integration assay either alone or in mixtures. IN derivatives contained the wild-type sequence (+), the D116N catalytic substitution ("N"), the S119A target site specificity substitution ("A"), or both substitutions ("NA"). Lane 1 depicts a negative control in which all steps were performed but no IN was added. Lane 24 depicts a negative control of the PCR only. (B) Quantitation of target site preference in the top strand of a phage lambda DNA target. To determine whether the reactions produced a wild-type or an S119A target site pattern, the ratio between the intensities of bands α and β (marked in panel A) within each lane was determined and graphed on the logarithmic scale underneath the gel lanes. $P = 0.0095$ for comparison of pooled + to pooled A values; Mann-Whitney test. (C) Assays of integration into the bottom strand of a phage lambda DNA target. Reaction conditions for each lane are marked as described for panel A. Lane 1 depicts a negative control of the PCR only. Lane 2 depicts a negative control in which all reaction steps were performed but no IN was added. (D) Quantitation of target site preference in the bottom strand of a phage lambda DNA target. The ratio between the intensities of bands γ and δ (marked in panel C) was determined and graphed on a logarithmic scale. $P = 0.0095$ for comparison of pooled + to pooled A values; Mann-Whitney test.

do this, we introduced the D116N and/or S119A substitutions into either 1-212 or 50-288 partners and then asked whether the determinant of target site selection was active in the catalytic (50-288) or the noncatalytic (1-212) background.

Reactions were first analyzed with single truncated INs (Fig. 3A, lanes 5 to 12, and C, lanes 6 to 13). As seen for the single truncation reactions shown in Fig. 2, IN truncations containing the D116N catalytic site substitution (Fig. 3A, lanes 6, 8, 10, and 12) did not yield any products, while INs with the wild-type residue at 116 did (Fig. 3A, lanes 5, 7, 9, and 11). Again, it is

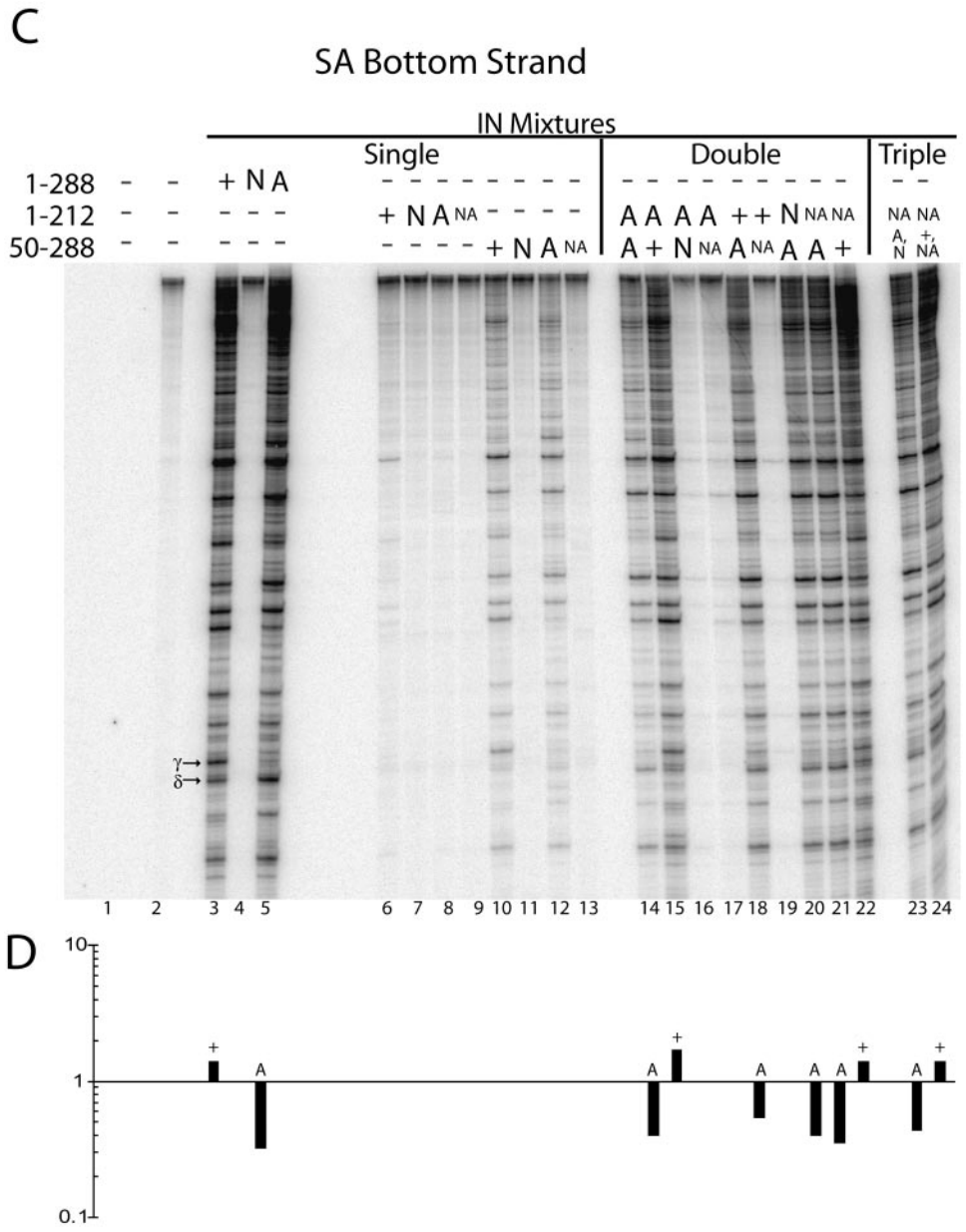

FIG. 3—*Continued.*

apparent that the 50-288 truncations have more activity by themselves than the 1-212 truncations. Thus, in complementing mixtures, interpretation is possible only when there is a higher level of product formation than with either single truncation alone.

Figure 3A, lanes 13 and 14, and C, lanes 14 and 15, show integration products from complementation assays where the 1-212 variant contained the S119A substitution and the 50-288 truncation was varied. When the 50-288 truncation contained the S119A substitution, the A pattern results, and when the 50-288 mutant is of the wild type, the + pattern results. Results for two strongly affected bands are quantified in Fig. 3B and D. When the 1-212 partner had the wild-type residue at 119, the pattern was nevertheless determined by the 50-288 partner (Fig. 3A, lane 17, and C, lane 18). When the 1-212 partner contained the D116N substitution, with or without S119A, the target site pattern was still determined by the genotype of the 50-288 partner. These findings indicate that the determinant of target site pattern is tracking with the active catalytic core domain on IN 50-288.

Modulation of target site specificity by the S119D substitution. The S119D substitution has also been shown to alter IN target site preferences but yields a pattern of preferred bands different from that seen for S119A mutants (34). IN variants containing the S119D substitution in the wild-type background ("D") alone and containing the D116N substitution as well ("ND") were tested for strand transfer activity and alterations in target site preference (Fig. 4). Figure 4A and C show that

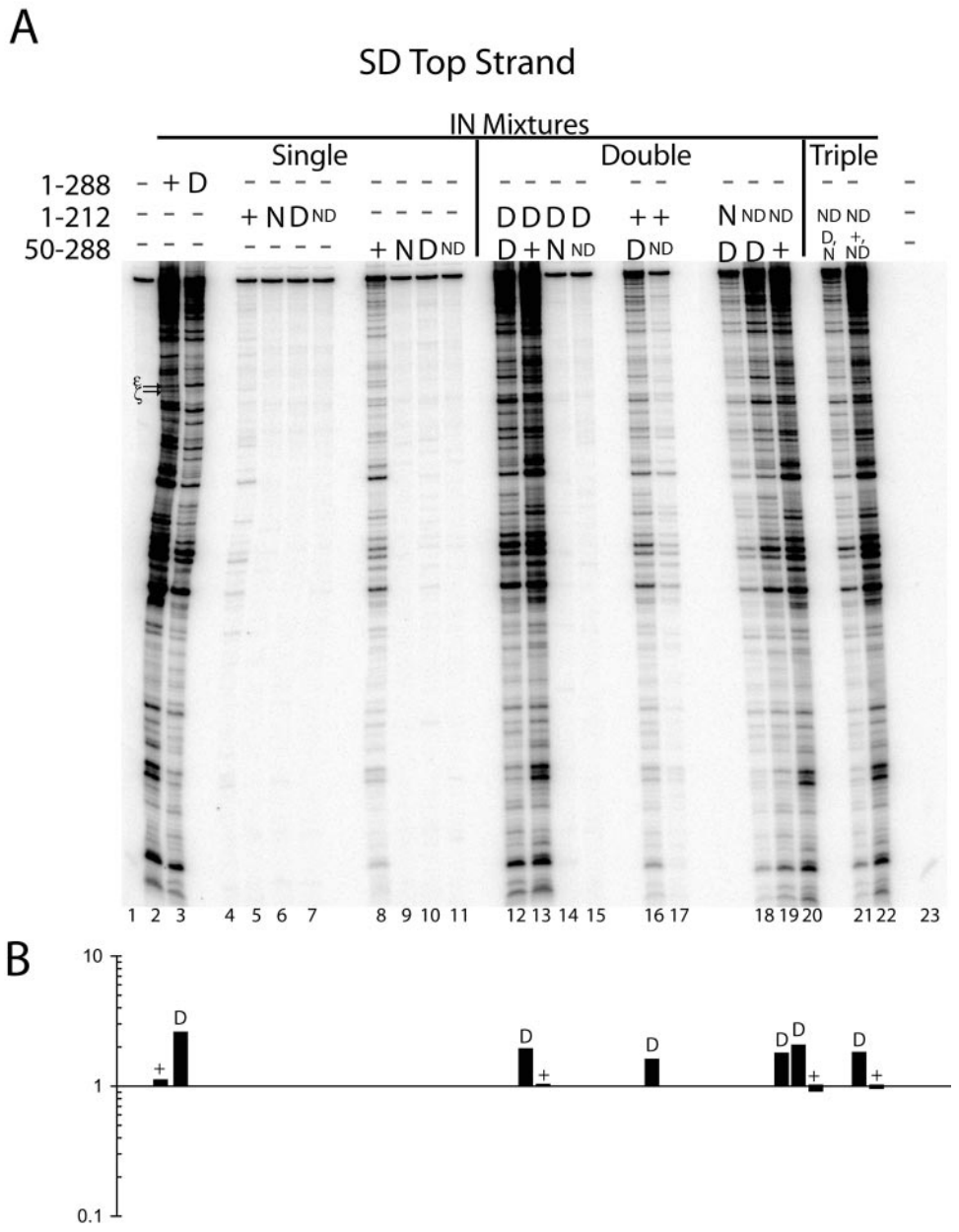

FIG. 4. Complementation assays in vitro containing S119D indicate that the 50–288 partner is responsible for both target sequence recognition and catalysis. (A) Assays of integration into the top strand of a phage lambda DNA target. The S119D target site specificity substitution ("D") and both substitutions together ("ND") are marked; other markings are as described for Fig. 3. Lane 1 depicts a negative control where all reaction steps were performed but no IN was added. Lane 23 depicts a negative control of the PCR only. (B) Quantitation of target site preference in the top strand of a phage lambda DNA target was carried out as described above for the ratio of ε to ζ. $P = 0.0095$ for comparison of pooled + to pooled D values; Mann-Whitney test. (C) Assays of integration into the bottom strand of a phage lambda DNA target. Reaction conditions for each lane are marked as described for panel A. Lanes 1 and 23 depict negative controls as described for panel A. (D) Quantitation of target site preference in the bottom strand of a phage lambda DNA target carried out as described above for the ratio of η to θ. $P = 0.0095$ for comparison of pooled + to pooled D values; Mann-Whitney test.

the wild type and S119D showed quite different patterns of favored target sites, and this is quantified in Fig. 4B and D. Target site selection also differed quite strongly between S119A and S119D, as can be seen by comparing Fig. 3 and 4.

Complementation assays were performed with the S119D mutants as for the S119A mutants. As was seen previously, single-truncation mutants were deficient in activity compared to the full-length mutants (Fig. 4A and C, lanes 4 to 11). The decrease in activity of the truncations containing S119D was more pronounced than the decrease seen for the wild-type truncations. This may be due to a decrease in target DNA binding by S119D, as proposed previously (34).

As with S119A, complementation assays with S119D showed that the target site pattern was determined by the residue at

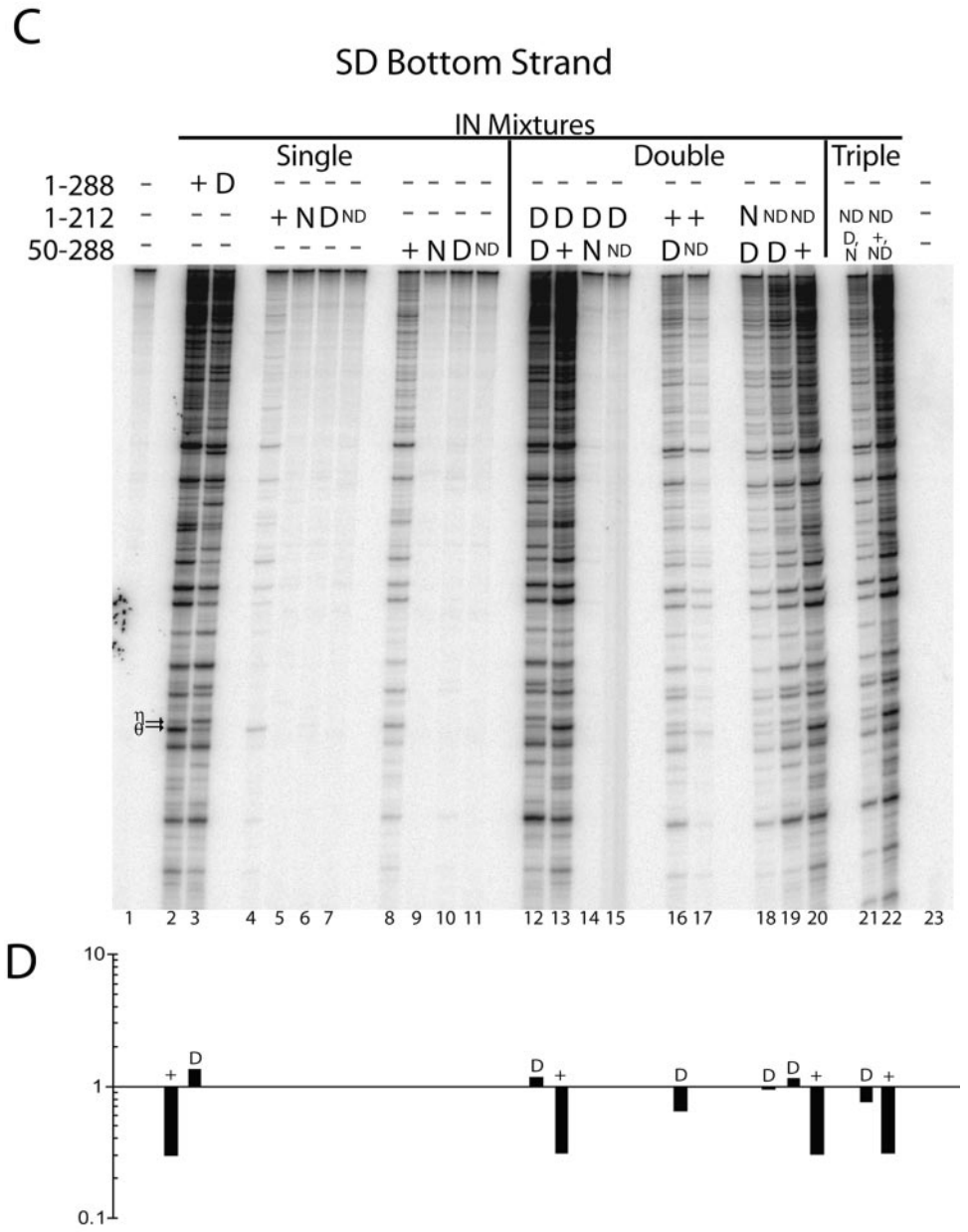

FIG. 4—*Continued.*

119 of the active IN 50-288 partner, regardless of which 1-212 IN variant was used. This is exemplified by comparison of lanes 12 and 13 in Fig. 4A or C, where there is a difference in the patterns of integration similar to what was seen for the 1-288 pattern variation between the + and D INs (Fig. 4A or C, lanes 2 and 3). Quantitation of the intensities of bands ε and ζ (Fig. 4A and B) or η and θ (Fig. 4C and D) revealed a significant difference in the band ratios for D and + with changes in the 50-288 subunit. Thus, results with S119D also indicated that both catalysis and target site specificity are carried out by the catalytic domain of the 50-288 partner.

In some pairs, reduced activity was seen in the presence of S119D, which complicated parts of the analysis. Specifically, a decrease in strand transfer capability was noted in samples where S119D was present in the 50-288 component but absent in the 1-212 variant. This was not seen when S119D was present only in the 1-212 truncation mutants. A simple model for these results is that the wild-type IN 1-212 bound DNA more tightly than IN 50-288 S119D, and IN 1-212 thus competed off the active 50-288 subunit.

Complementation assays using simple oligonucleotide substrates. We also verified the results from the PCR-based in vitro integration assay using oligonucleotide-based substrates as in previous studies of complementation in vitro (13, 43). In these assays, an oligonucleotide duplex substrate models the viral DNA end, and another oligonucleotide duplex of the same sequence functions as the target DNA (Fig. 1A). As expected, all IN variants that contained intact catalytic do-

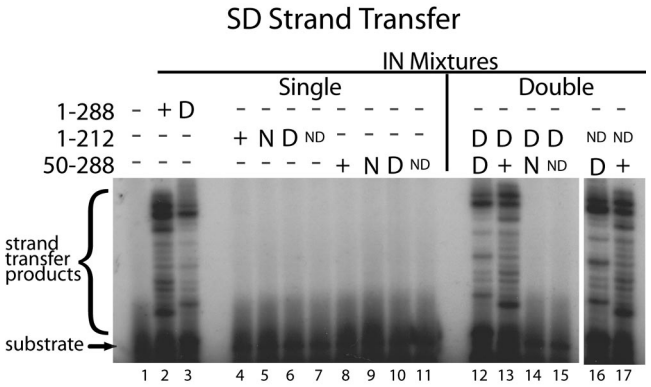

FIG. 5. Complementation assay using oligonucleotide-based substrates in the presence of S119D. Strand transfer activity of full-length (1–288), C-terminally truncated (1–212), or N-terminally truncated (50–288) IN variants containing wild-type sequence (+), D116N ("N"), S119D ("D"), or D116N and S119D ("ND") was measured with end-labeled substrates. Proteins were analyzed either individually or in double mixtures of 1–212 and 50–288 proteins. The 30-nucleotide substrate DNA and strand transfer products are labeled.

mains (e.g., without D116N) were able to carry out the permissive disintegration reaction (data not shown), indicating that the catalytic domains were functional.

Unfortunately, the diminished activity of the S119A/D mutants made some of these reactions difficult to analyze. Therefore, Fig. 5 shows the subset of complementing pairs that gave interpretable results. As seen in lanes 2 and 3, a ladder of ^{32}P-labeled bands is seen above the 30-nucleotide substrate, indicating strand transfer. The patterns of strand transfer in these reactions differ between the + and D full-length mutants. Lanes 4 to 11 contain products from assays with a single truncated IN and, as expected, these enzymes showed no strand transfer activity. The complementing mixtures in lanes 12 to 17 contained strand transfer products only when an active catalytic domain was present in the IN 50-288 partner. The pattern of target site selection was again associated with the genotype of the active catalytic domain on the 50-288 IN fragment. Similar results were also seen with this assay when the S119A substitution was used (data not shown).

Complementing mixtures with three different truncations. Several models could account for our observations thus far. In one, the same 50-288 monomer is directing both target site selection and catalysis. For example, a heterodimer composed of one 1-212 and one 50-288 could form the complex active at the viral DNA end tested in our assays. Alternatively, a higher-order complex could form, but a single 50-288 monomer still contributes both functions. However, it is also possible that a higher-order complex forms, and one 50-288 monomer contributes catalytic activity, while another 50-288 monomer contributes the target site selection activity.

In order to examine this issue, we analyzed the effect of adding two different 50-288 derivatives into a reaction mixture with a catalytically inactive IN 1-212. For the most informative reactions, a 1-212 truncation containing the D116N catalytic substitution was mixed with (i) a 50-288 truncation with D116N and (ii) a 50-288 truncation with an active catalytic domain. The 50-288 truncations also had different target site-specifying residues at 119. In these reactions, if a single catalytic domain within the multimer is carrying out both catalysis and target site selection, then the target site selection pattern will follow the genotype at residue 119 of the active 50-288 monomer. If different 50-288 monomers with different residues at 119 are carrying out the two activities, then the target site pattern would be a mixture due to the formation of mixed multimers.

Reactions were conducted with (i) a 1-212 derivative with D116N and S119A, (ii) a 50-288 derivative with D116N, and (iii) a 50-288 derivative with S119A (Fig. 3A, lane 22, and C, lane 23). In these reactions, if catalysis and target site selection were being controlled by the same IN 50-288 monomer, we would expect to see the S119A target site pattern. If multimers with two or more IN 50-288 derivatives are the active form and if catalysis and target site selection were being controlled by different IN 50-288 monomers, we would expect to see a mixture of A and + target site patterns. This mixture had a clear A pattern and matched products seen when the catalytically inactive 50-288 truncation was not included (Fig. 3A, lane 20, and Fig. 3C, lane 21; quantitated in B and D). These data support a model in which, at this single long terminal repeat (LTR) end, target site specificity and catalysis are being dictated by the same IN 50-288 monomer within the IN multimer.

Triple mixtures were also made containing (i) a 1-212 truncation with D116N and S119A, (ii) a wild-type 50-288 truncation, and (iii) a 50-288 truncation with D116N and S119A. This mixture displayed a + target site pattern (Fig. 3A, lane 23, and C, lane 24; quantitated in B and D). Identical patterns were seen for reaction mixtures lacking the catalytically inactive IN 50-288 protein (Fig. 3A, lane 21, and C, lane 22). These findings indicate that the 119 genotype of the 50-288 monomer contributing the active catalytic site determines the pattern of target site selection.

A confounding alternative explanation for these results would be that the D116N substitution used to block catalysis itself diminished target DNA binding, so that the D116N-containing IN could not participate in target selection in our reactions. Arguing against this idea is the observation that addition of IN derivatives containing D116N to complementing mixtures reduced product formation in several types of assays, consistent with competition for binding to substrate DNA. In fact, the D116N-modified mutants were consistently better competitors than the S119D mutant, the latter having been proposed to diminish target DNA binding (34). These data argue that the D116N substitution does not strongly reduce DNA binding and so is suitable as a probe in the assays reported here.

Similar results were obtained with triple mixtures containing the S119D substitution in place of the S119A substitution (Fig. 4A and C, lanes 21 and 22). In these assays also, the target site pattern followed that of the S119 variant in the 50-288 subunit containing the active catalytic core domain. Thus, in reactions using either S119A or S119D as probes, we found that target site selection tracked with the active 50-288 partner. Altogether, these results support the hypothesis that catalysis and target site specificity at a single viral DNA end are controlled by a single catalytic domain within an IN 50-288 monomer.

DISCUSSION

Here we examine the functions of specific HIV IN monomers within the active IN multimer. Truncated IN derivatives,

each inactive for strand transfer on its own, can display terminal cleavage and strand transfer activities in complementing mixtures (references 13 and 43 and this work). In this study, we have used such complementation assays to determine the relationship between the subunit carrying out catalysis and that mediating target site selection. Residues associated with catalysis and target site specificity both reside in the catalytic core domain, but it had been previously unknown whether two separate catalytic domains contribute these functions within a multimer or whether a single catalytic domain does both. In this study, we have constructed truncated IN derivatives containing catalytic (D116N) or target site selection (S119A/D) substitutions and used them in complementation studies pairwise or in triple combinations. Our findings support a model in which a single monomer contributes both functions.

Evidence that the same IN 50-288 monomer contributes catalytic activity and target site specificity in triple mixes. In order to investigate whether the same 50-288 monomer within the IN complex is carrying out catalysis and target site selection, as opposed to the possibility that two different 50-288 monomers are contributing the two functions, we tested complementation in triple IN mixtures (Fig. 3 and 4). These mixtures contained a catalytically inactive 1-212 truncation and two different 50-288 truncations where one of the two contained D116N. In addition, one 50-288 truncation contained S119A or S119D. In these reactions, if catalysis and target site selection at one viral LTR end were being controlled by different IN 50-288 monomers, one would expect to see a mixture of the wild-type and S119A or S119D target site patterns; that is, if catalysis and target site selection were being controlled by the same IN 50-288 monomer, the target site pattern would be that dictated by the genotype at residue 119 in the active 50-288 derivative. We consistently found the target site pattern was that expected for the catalytically active IN 50-288 variant and not a mixture. We interpret this as indicating that catalysis and target site specificity at a single viral LTR end are being dictated by the same 50-288 catalytic domain monomer within a multimer.

The amino acid substitutions at residue 119 (or at the corresponding residue 124 in Rous sarcoma virus IN) result in an alteration of target site specificity but do not strictly specify this as a point of direct contact with the target DNA. However, the previous finding that substitution of Ser for Asp promotes terminal cleavage while diminishing strand transfer is readily explained by the direct binding of Ser to the DNA target and interference with binding by Asp. In addition, in the presence of the Asp substitution, nonspecific DNA cleavage by IN is diminished, and IN-DNA binding becomes more salt sensitive (34). Thus, we favor the view that the 119 position in HIV directly contacts target DNA, and that both viral and target DNA bind a single catalytic domain monomer, but more data on the nature of the 119 contact would be helpful.

The nature of the active IN multimer has not been fully clarified. Because the two ends of the viral DNA must be integrated into target DNA, it seems likely from symmetry considerations that there are an even number of monomers involved. The strongest dimerization contact seen structurally is in the catalytic domain, but this places the active sites in a relationship unsuited to joining the two viral DNA ends with the correct spacing (11). Thus, it seems likely that a tetrameric

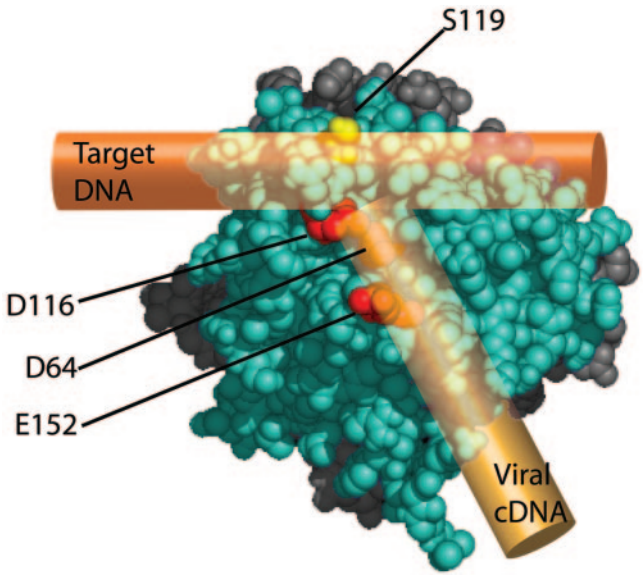

FIG. 6. Model for interaction between the IN catalytic core domain, viral LTR, and target DNA. The structure of a core domain dimer is shown with one core domain monomer (cyan) containing the active catalytic triad (red) and interacting with both the target (copper cylinder) and viral (gold cylinder) DNAs. The S119 residue (yellow) is also marked. Coordinates are from 1BIU.pdb (21). The protein structure in this figure was made using the PyMOL Molecular Graphics System (Delano Scientific LLC).

structure is involved. Previous work indicated that at least two IN monomers act at each viral DNA end (18, 29). IN-DNA cross-linking indicated that an IN monomer contacted position 7 in the viral DNA via contacts with the C-terminal domain, and another monomer contributed the catalytic site (18). Work presented here suggests that the same catalytic monomer also binds the target DNA. A variety of interwoven tetrameric models that meet these constraints can be proposed (18, 39, 45).

Model for catalytic domain-DNA interactions. The observation that catalysis and target site specificity are being determined at each viral LTR end by the same monomer specifies in more detail the array of DNA ligands at the catalytically relevant core domain. Figure 6 models a dimer of the 50-212 IN catalytic domain (11, 21) in complex with viral cDNA and target DNA. The active monomer is shown in cyan, and its catalytic triad (D64, D116, and E152) is highlighted in red. The viral cDNA was placed so that the 5′ end dinucleotide is in close proximity to residue 148, which has been shown to interact with the DNA in cross-linking studies (16, 20). The viral cDNA was also drawn in a basic cleft hypothesized to be the viral cDNA binding tract (11, 18, 21). The target DNA has been placed so that it can interact with the viral cDNA near the catalytic residues and be in close proximity to S119 (shown in yellow). We note, however, that S119 provides only a single tethering point, so there is uncertainty in the rotational position of the target DNA about S119 on IN. A key new point in this model is that a single core domain monomer can now be specified as interacting with the two DNAs during catalysis.

Understanding IN inhibition and drug resistance. These findings may be useful for understanding IN inhibitors and

mechanisms of drug resistance. The diketo acid and the related naphthyridine classes of IN inhibitors are the only compounds convincingly shown so far to inhibit IN in vivo (26, 27). These inhibitors selectively block strand transfer by blocking target DNA binding (15, 26) while still permitting terminal cleavage, as with the S119D substitution. Structural studies, modeling, and mapping of viral escape mutants have all indicated that these compounds bind near the active site on the catalytic domain. An attractive model is that the inhibitors bind to the catalytically relevant monomer identified here, which in turn raises several mechanistic questions. Might the inhibitors make contact with the viral DNA end or metal atoms stabilized by binding the viral DNA as well as with IN itself? Might IN conformational changes induced by the nearby binding of the viral DNA stabilize inhibitor binding? Some of the amino acid substitutions that result in IN inhibitor resistance are rather distant from S119 but potentially near the viral DNA end—might these act indirectly by altering the position of the viral DNA? Future studies will be needed to address these questions. The complementation methods reported here should be applicable in addressing an important question concerning resistance: must the amino acid substitutions conferring drug resistance reside on the catalytically relevant IN monomer identified here, or might they reside on a different monomer?

ACKNOWLEDGMENTS

We thank members of the Bushman laboratory for helpful discussions and Greg Van Duyne for the gift of the pDuetMxe vector.

This work was supported by NIH grants AI34786 and GM068408, the James B. Pendleton Charitable Trust, and Robin and Frederic Withington. T.L.D. was supported by T32-AI-07632 (Training Grant in HIV Pathogenesis).

REFERENCES

1. **Appa, R. S., C. G. Shin, P. Lee, and S. A. Chow.** 2001. Role of the nonspecific DNA-binding region and alpha helices within the core domain of retroviral integrases in selecting target DNA sites for integration. J. Biol. Chem. **276:**45848–45855.
2. **Baker, T. A., M. Mizuuchi, H. Savilahti, and K. Mizuuchi.** 1993. Division of labor among monomers within the Mu transposase tetramer. Cell **74:**723–733.
3. **Bushman, F. D.** 2001. Lateral DNA transfer: mechanisms and consequences. Cold Spring Harbor Laboratory Press, Cold Spring Harbor, N.Y.
4. **Bushman, F. D.** 1994. Tethering human immunodeficiency virus 1 integrase to a DNA site directs integration to nearby sequences. Proc. Natl. Acad. Sci. USA **91:**9233–9237.
5. **Bushman, F. D., A. Engelman, I. Palmer, P. Wingfield, and R. Craigie.** 1993. Domains of the integrase protein of human immunodeficiency virus type 1 responsible for polynucleotidyl transfer and zinc binding. Proc. Natl. Acad. Sci. USA **90:**3428–3432.
6. **Chen, J. C.-H., J. Krucinski, L. J. W. Miercke, J. S. Finer-Moore, A. H. Tang, A. D. Leavitt, and R. M. Stroud.** 2000. Crystal structure of the HIV-1 integrase catalytic core and C-terminal domains: a model for viral DNA binding. Proc. Natl. Acad. Sci. USA **97:**8233–8238.
7. **Chen, Z., Y. Yan, S. Munshi, Y. Li, J. Zugay-Murphy, B. Xu, M. Witmer, P. Felock, A. Wolfe, V. Sardana, E. A. Emini, D. Hazuda, and L. C. Kuo.** 2000. X-ray structure of simian immunodeficiency virus integrase containing the core and C-terminal domain (residues 50–293)—an initial glance of the viral DNA binding platform. J. Mol. Biol. **296:**521–533.
8. **Chow, S. A., K. A. Vincent, V. Ellison, and P. O. Brown.** 1992. Reversal of integration and DNA splicing mediated by integrase of human immunodeficiency virus. Science **255:**723–726.
9. **Coffin, J. M., S. H. Hughes, and H. E. Varmus (ed.).** 1997. Retroviruses. Cold Spring Harbor Laboratory Press, Cold Spring Harbor, N.Y.
10. **Craig, N. L., R. Craigie, M. Gellert, and A. M. Lambowitz (ed).** 2002. Mobile DNA II. ASM Press, Washington, D.C.
11. **Dyda, F., A. B. Hickman, T. M. Jenkins, A. Engelman, R. Craigie, and D. R. Davies.** 1994. Crystal structure of the catalytic domain of HIV-1 integrase: similarity to other polynucleotidyl transferases. Science **266:**1981–1986.
12. **Engelman, A.** 1999. *In vivo* analysis of retroviral integrase structure and function Adv. Virus Res. **52:**411–426.
13. **Engelman, A., F. D. Bushman, and R. Craigie.** 1993. Identification of discrete functional domains of HIV-1 integrase and their organization within an active multimeric complex. EMBO J. **12:**3269–3275.
14. **Engelman, A., and R. Craigie.** 1992. Identification of conserved amino acid residues critical for human immunodeficiency virus type 1 integrase function in vitro. J. Virol. **66:**6361–6369.
15. **Espeseth, A. S., P. Felock, A. Wolfe, M. Witmer, J. Grobler, N. Anthony, M. Egbertson, J. Y. Melamed, S. Young, T. Hamill, J. L. Cole, and D. J. Hazuda.** 2000. HIV-1 integrase inhibitors that compete with the target DNA substrate define a unique strand transfer conformation for integrase. Proc. Natl. Acad. Sci. USA **97:**11244–11249.
16. **Esposito, D., and R. Craigie.** 1998. Sequence specificity of viral end DNA binding by HIV-1 integrase reveals critical regions for protein-DNA interaction. EMBO J. **17:**5832–5843.
17. **Fletcher, T. M., M. A. Soares, S. McPhearson, H. Hui, M. Wiskerchen, M. A. Muesing, G. M. Shaw, A. D. Leavitt, J. D. Boeke, and B. H. Hahn.** 1997. Complementation of integrase functions in HIV-1 virions. EMBO J. **16:**5123–5138.
18. **Gao, K., S. L. Butler, and F. D. Bushman.** 2001. Human immunodeficiency virus type 1 integrase: arrangement of protein domains in active cDNA complexes. EMBO J. **20:**3565–3576.
19. **Gao, K., S. Wong, and F. Bushman.** 2004. Metal binding by the $D,DX_{35}E$ motif of human immunodeficiency virus type 1 integrase: selective rescue of Cys substitutions by Mn^{2+} in vitro. J. Virol. **78:**6715–6722.
20. **Gerton, J. L., S. Ohgi, M. Olsen, J. Derisi, and P. O. Brown.** 1998. Effects of mutations in residues near the active site of human immunodeficiency virus type 1 integrase on specific enzyme-substrate interactions. J. Virol. **72:**5046–5055.
21. **Goldgur, Y., F. Dyda, A. B. Hickman, T. M. Jenkins, R. Craigie, and D. R. Davies.** 1998. Three new structures of the core domain of HIV-1 integrase: an active site that binds magnesium. Proc. Natl. Acad. Sci. USA **95:**9150–9154.
22. **Greenwald, J., V. Le, S. L. Butler, F. D. Bushman, and S. Choe.** 1999. Mobility of an HIV-1 integrase active site loop is correlated with catalytic activity. Biochemistry **38:**8892–8898.
23. **Guo, F., D. N. Gopaul, and G. D. Van Duyne.** 1997. Structure of Cre recombinase complexed with DNA in a site-specific recombination synapse. Nature **398:**40–46.
24. **Harper, A. L., L. M. Skinner, M. Sudol, and M. Katzman.** 2001. Use of patient-derived human immunodeficiency virus type 1 integrases to identify a protein residue that affects target site selection. J. Virol. **75:**7756–7762.
25. **Harper, A. L., M. Sudol, and M. Katzman.** 2003. An amino acid in the central catalytic domain of three retroviral integrases that affects target site selection in nonviral DNA. J. Virol. **77:**3838–3845.
26. **Hazuda, D. J., N. J. Anthony, R. P. Gomez, S. M. Jolly, J. S. Wai, L. Zhuang, T. E. Fisher, M. Embrey, J. P. Guare, Jr., M. S. Egbertson, J. P. Vacca, J. R. Huff, P. J. Felock, M. V. Witmer, K. A. Stillmock, R. Danovich, J. Grobler, M. D. Miller, A. S. Espeseth, L. Jin, I. W. Chen, J. H. Lin, K. Kassahun, J. D. Ellis, B. K. Wong, W. Xu, P. G. Pearson, W. A. Schleif, R. Cortese, E. Emini, V. Summa, M. K. Holloway, and S. D. Young.** 2004. A naphthyridine carboxamide provides evidence for discordant resistance between mechanistically identical inhibitors of HIV-1 integrase. Proc. Natl. Acad. Sci. USA **101:**11233–11238.
27. **Hazuda, D. J., P. Felock, M. Witmer, A. Wolfe, K. Stillmock, J. A. Grobler, A. Espeseth, L. Gabryelski, W. Schleif, C. Blau, and M. D. Miller.** 2000. Inhibitors of strand transfer that prevent integration and inhibit HIV-1 replication in cells. Science **287:**646–650.
28. **Heuer, T. S., and P. O. Brown.** 1997. Mapping features of HIV-1 integrase near selected sites on viral and target DNA molecules in an active enzyme-DNA complex by photo-cross-linking. Biochemistry **36:**10655–10665.
29. **Heuer, T. S., and P. O. Brown.** 1998. Photo-cross-linking studies suggest a model for the architecture of an active human immunodeficiency virus type-1 integrase-DNA complex. Biochemistry **37:**6667–6678.
30. **Jenkins, T. M., A. Engelman, R. Ghirlando, and R. Craigie.** 1996. A soluble active mutant of HIV-1 integrase: involvement of both the core and carboxyl-terminal domains in multimerization. J. Biol. Chem. **271:**7712–7718.
31. **Katzman, M., and M. Sudol.** 1998. Mapping viral DNA specificity to the central region of integrase by using functional human immunodeficiency virus type 1/visna virus chimeric proteins. J. Virol. **72:**1744–1753.
32. **Katzman, M. K., and M. Sudol.** 1995. Mapping domains of retroviral integrase responsible for viral DNA specificity and target site selection by analysis of chimeras between human immunodeficiency virus type 1 and visna virus type 1 and visna virus integrases. J. Virol. **69:**5687–5696.
33. **Kitamura, Y., Y. M. Lee, and J. M. Coffin.** 1992. Nonrandom integration of retroviral DNA *in vitro*: effect of CpG methylation. Proc. Natl. Acad. Sci. USA **89:**5532–5536.
34. **Konsavage, W. M., Jr., S. Burkholder, M. Sudol, A. L. Harper, and M. Katzman.** 2005. A substitution in Rous sarcoma virus integrase that separates its two biologically relevant enzymatic activities. J. Virol. **79:**4691–4699.
35. **Lee, J., M. Jayaram, and I. Grainge.** 1999. Wild-type Flp recombinase cleaves DNA in trans. EMBO J. **18:**784–791.
36. **Lu, R., A. Limon, E. Devroe, P. A. Silver, P. Cherepanov, and A. Engelman.**

2004. Class II integrase mutants with changes in putative nuclear localization signals are primarily blocked at a postnuclear entry step for human immunodeficiency virus type 1 replication. J. Virol. **78:**12735–12746.
37. **Lu, R., A. Limon, H. Z. Ghory, and A. Engelman.** 2005. Genetic analyses of DNA-binding mutants in the catalytic core domain of human immunodeficiency virus type 1 integrase. J. Virol. **79:**2493–2505.
38. **Mizuuchi, M., T. A. Baker, and K. Mizuuchi.** 1995. Assembly of phage Mu transpososomes: cooperative transitions assisted by protein and DNA scaffolds. Cell **83:**375–385.
39. **Podtelezhnikov, A. A., K. Gao, F. D. Bushman, and A. McCammon.** 2003. Modelling HIV-1 integrase complexes based on their hydrodynamic structure. Biopolymers **68:**110–120.
40. **Pryciak, P. M., and H. E. Varmus.** 1992. Nucleosomes, DNA-binding proteins, and DNA sequence modulate retroviral integration target site selection. Cell **69:**769–780.
41. **Shibagaki, Y., and S. A. Chow.** 1997. Central core domain of retroviral integrase is responsible for target site selection. J. Biol. Chem. **272:**8361–8369.
42. **van Gent, D. C., A. A. M. Oude Groeneger, and R. H. A. Plasterk.** 1992. Mutational analysis of the integrase protein of human immunodeficiency virus type 2. Proc. Natl. Acad. Sci. USA **89:**9598–9602.
43. **van Gent, D. C., C. Vink, A. A. M. Oude Groeneger, and R. H. A. Plasterk.** 1993. Complementation between HIV integrase proteins mutated in different domains. EMBO J. **12:**3261–3267.
44. **Vink, C., A. M. Oude Groeneger, and R. H. A. Plasterk.** 1993. Identification of the catalytic and DNA-binding region of the human immunodeficiency virus type 1 integrase protein. Nucleic Acids Res. **21:**1419–1425.
45. **Wang, J. Y., H. Ling, W. Yang, and R. Craigie.** 2001. Structure of a two-domain fragment of HIV-1 integrase: implications for domain organization in the intact protein. EMBO J. **20:**7333–7343.
46. **Yang, Z. N., T. C. Mueser, F. D. Bushman, and C. C. Hyde.** 2000. Crystal structure of an active two-domain derivative of rous sarcoma virus integrase. J. Mol. Biol. **296:**535–548.